Journal of Aeronautics and Space Technologies

16(1) (2023) 1-14

Journal Homepage: jast.hho.msu.edu.tr

RESEARCH ARTICLE

Optimization of Induction Heating Coil in the Surface Hardening Process

Yüzey Sertleştirme İşleminde İndüksiyon Bobininin Eniyilemesi

Yalın Yamaç[1], Beril Özçelik[2*],

[1] *Kahramanmaras Sutcu Imam University, Faculty of Engineering and Architecture, Department of Mechanical Engineering, 46050 Kahramanmaras, Turkey*

[2] *Kahramanmaras Sutcu Imam University, Faculty of Engineering and Architecture, Department of Mechanical Engineering, 46050 Kahramanmaras, Turkey*

Received: *July 10, 2022* ***Revised:*** *August 10, 2022* ***Accepted:*** *August 17, 2022*

Abstract

Induction surface hardening, which is used in various fields in the aerospace industry, is an important technology due to its accuracy, repeatability and energy efficiency. By modeling this heat treatment, the process parameters and efficiencies will be understood and its effective use in critical aircraft application areas will be expanded by contributing to the development of this technology. In this study, the induction surface hardening process of the cylindrical sample from AISI 4340 steel is simulated using couple field analysis. The coil geometry is optimized using two approaches to achieve homogeneous temperature distribution on the heated sample surface. One is to change the diameter of the coil rings and the other is to change the interval of the coil rings. After the diameters of the coil rings optimization, uniformity is achieved at the sample surface temperature, with deviations up to ±4°C from the austenitizing temperature. After the intervals of the coil rings optimization, homogenous temperature distribution is achieved at the sample surface temperature, and deviations from the austenitizing temperature are up to ±3°C. The current value required for heating the sample surface to the austenitizing temperature in 2s has been reduced, and energy saving have been obtained.

Keywords: Electromagnetic Field, Finite Elements Method, Induction Heating, Optimization, Temperature Distribution, Surface Hardening.

Özet

Havacılık ve uzay sanayisinde çeşitli alanlarda kullanılan indüksiyonla sertleştirme, doğruluğu, tekrarlanabilirliği, enerji verimliliği nedeniyle önemli bir teknolojidir. Bu ısıl işlemin modellenmesi ile işlem parametreleri ve etkileri anlaşılacak ve bu teknolojinin geliştirilmesine katkı sağlanarak kritik uçak uygulama alanlarında etkin kullanımı yaygınlaştırılacaktır. Bu çalışmada, AISI 4340 çelik malzemeden, silindirik geometriye sahip numunenin indüksiyonla yüzey sertleştirmesinin birleşik çözümleme ile benzetimi yapılmıştır. Isıtılmış numune yüzeyinde homojen sıcaklık dağılımı elde etmek için bobin geometrisi iki yaklaşım kullanılarak eniyilenmiştir. Bunlardan ilki bobin halkalarının çapını değiştirmek diğeri ise bobin halkalarının aralığını değiştirmektir. Bobin halkalarının çapları eniyileştirildiğinde, numune yüzey sıcaklığında tekdüzelik yakalanmış, östenitleme sıcaklığından ±4°C' ye kadar sapmalar olmuştur. Bobin halkalarının aralıkları optimize edildiğinde numune yüzey sıcaklığında yine düzgün sıcaklık dağılımı sağlanmış, östenitleme sıcaklığından ±3°C' ye kadar sapmalar olmuştur. Yapılan eniyilemeler sonrasında, numune yüzeyini östenitleme sıcaklığına 2 sn. sürede ısıtma için gerekli olan akım değeri düşürülmüş, enerjiden de tasarruf sağlanmıştır.

Anahtar Kelimeler: Elektromanyetik Alan, Sonlu Ögeler (Elemanlar) Yöntemi, İndüksiyonla Isıtma, Eniyileme, Sıcaklık Dağılımı, Yüzey Sertleştirme.

*Corresponding Author
E-mail: bozcelik@ksu.edu.tr

1. INTRODUCTION

Electromagnetic field principles defined in Maxwell's equations are used in the induction heating method. During the method, electrically conductive material is located in the variable electromagnetic field created by an induction coil through which alternating current is flowing. As a result of electromagnetic induction, eddy currents are induced in the heated material, which have the opposite direction to the current in the induction coil. Heating consists of resistance and hysteresis losses of the material. The heat is generated directly inside the material without any mechanical contact with the heated object and the coil. The method has been preferred for the last fifty years because it can provide high heating rate (such as 800°C/s and above) and heat electrically conductive materials such as metal in a fast, efficient and non-contact way [1-3]. Induction heating has become a popular method in various and different applications such as mass heating and melting in the industry, heat treatments, welding, soldering, shrink fitting joints, plastic deformation, and hyperthermia treatment in the medical sector [3-5]. Surface hardening is one of the induction heat treatments. In cases where hardness is not desired in the whole part, surface hardening can be done by induction only by phase transformation without changing the composition of the material surface. The reproducibility and reliability of the results, theoretically and experimentally, have made induction surface hardening an important area of use in the aerospace industry. Modeling this heat treatment process is a crucial factor that will enable the application of certain process parameters and understanding of the process, allowing this technology to be developed for power transmission shafts and gears, aircraft landing gears, heavily loaded elements of the aircraft engine and other aircrafts structural elements [6, 7].

In surface hardening, the surface layer of the sample is heated to a temperature above A_{c3} or A_{cm}, depending on the carbon ratio of a steel material, until austenitic structure obtained. Immediately after, the heated sample is rapidly cooled with a suitable cooling liquid (water, oil or polymer liquid). As a result, a harder and brittle martensitic structure is obtained in the hardened layer. The structure of inner part of the sample body does not change. The fact that the temperature at which the austenite structure is formed is not the same in all regions of the sample surface so different austenitizing temperature causes different cooling periods at those points. According to the Continuous Cooling Diagram of steel, these different cooling periods cause different microstructure in the sample. Martensitic structure can be observed in regions that cool at a rate above the critical cooling rate, and bainite, perlite or ferrite formation can be observed in regions that cool more slowly due to incomplete hardening process [8].

The depth of the induction heated zone depends on the frequency of the alternating current, because of the skin effect, as well as the heat conduction property of the material. The magnetic field of the coil is also effective on the current paths and power density distribution due to the proximity relationship of the coils. In shortly, it becomes more complex to control the homogeneity of temperature in the heated zone due to the skin effect and proximity relationship [9].

In this study, with the optimization made to the coil geometry, a certain area of the sample surface is heated to the target temperature, and a homogeneous temperature have been tried to be obtained in the layer to be hardened. After quenching process, the same microstructure and the same hardness can be achieved on the sample surface. In the ideal case, the constant temperature of the target heating zone will ensure a homogeneous microstructure, while at the same time providing the least energy consumption. In the literature, there are studies for different applications to achieve homogeneous temperature distribution in the induction heating. For example, in the chemical vapor deposition method, optimizations have been made by changing the geometry of the susceptor, wafer, and the induction coil arrangement to obtain a homogeneous temperature distribution on the susceptor. Mei et al. created an air gap between the alumina and graphite susceptor and placed a heat transfer orbit for temperature distribution optimization in a vapor deposition [8]. The temperature difference in the susceptor had been reduced from 122.9 °C to 58.6 °C. Li et al. improved the uniformity of the temperature distribution in the wafer by 85.1% by creating V-shaped voids inside the susceptor in an induction heated vapor deposition reactor [9]. However, they stated that due to the v-shape, the heating efficiency decreased by 3.7% compared to the conventional gapless susceptor geometry. Li et al. improved the temperature distribution homogeneity of the T-shaped susceptor geometry used in a vapor deposition by extending the heat transfer line vertically, expanding it horizontally and creating a cylindrical hole under the susceptor [10]. Barka et al. simulated the induction heating of a bearing shoulder made of AISI 4340 steel with a finite element software [11]. Two washers of the same material adjacent to the heated area were added to make the temperature distribution more homogeneous on the surface. However, they achieved the homogeneity in the corner part by changing the coil geometry. Kucharski et al. achieved uniform temperature distribution in papermaking machines to dry tape-shaped materials using a series of independent inductors placed in such a way as to occupy the maximum area of the cylinder [12]. Fraczyk et al. controlled inductor positioning using two different algorithms which improved temperature control accuracy and temperature uniformity of sample surface [13]. Barglik et al. modeled induction hardening of gear wheels and examined temperature distribution of surface of a tooth [14]. Zhao et al. developed the modeling of induction heated gears and explored the effect of the number of iterative heating on the uniformity of temperature distribution in a bevel gear [15].

Changing the geometry of the workpiece in order to obtain a homogeneous temperature distribution on the workpiece surface is not easy in practice. In cases where the geometry of the workpiece cannot be changed, optimization can be made with the coil parameters. Coil optimization can be done in two ways. One of them is to design a different current value to pass through each coil ring. This will require adding a separate current control for each return to the system and will not be an economical solution. Instead of this, it would be more advantageous in practice to change the geometry of the coils when using a single current control for all coils. In this study, the heated surface of a cylindrical sample made of AISI 4340 steel for surface hardening was determined as the target surface. In order to obtain a constant temperature distribution on this target

surface, geometric optimization of the arrangement of the coil rings has been made using the finite element method. In the first case, the diameters of the coil rings are optimized; in the second case the intervals of the coil rings are optimized.

2. METHODOLOGY

2.1. Finite Element Model

The numerical model of the optimization is created in the Comsol Multiphysics software using the finite element method. The schematic view of the model is shown in Figure 1. 100 mm diameter, 500 mm long cylindrical steel sample is housed in a 10-rings copper coil with a diameter of 200 mm. The diameter of the copper tube used in the coil is 10 mm.

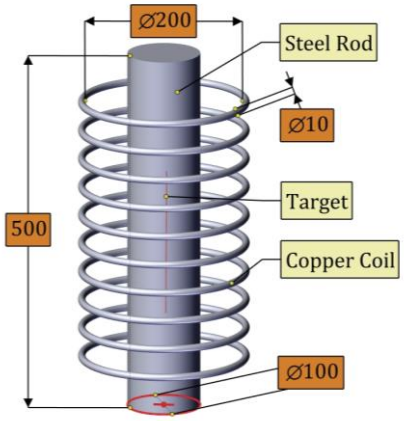


Figure 1. Schematic view of the model (mm).

AISI 4340 steel is chosen as the cylindrical sample material to be heated by induction. AISI 4340 steel is used in many applications where good mechanical and magnetic properties are required at low cost and offers good hardenability when subjected to quenching and tempering [16]. The material properties used in the finite element model of AISI 4340 steel are shown in Table 1.

Table 1. Properties of AISI 4340 steel.

Property	Value	Unit
Relative permeabilite	1	1
Electrical conductivity	4.032×10^6	S/m
Heat capacity	475	J/(kg·K)
Relative permittivity	1	1
Density	7850	kg/m^3
Thermal conductivity	44.5	W/(m·K)

In induction heating, the current frequency, current density, heating time and heat transfer parameters will affect the temperature distribution of sample. Induction heating is a coupling analysis and the physical properties of the heated sample will change with temperature. During the heating process, the resistivity and magnetic permeability of the heated material will change with temperature. Assuming the magnetic field strength is constant, the relative magnetic permeability of steel gradually decreases with increasing temperature and drops sharply near the curie point [17]. Ferromagnetic materials lose their ferromagnetic properties at temperatures above the curie point [14]. In the calculations, the relative magnetic permeability value of AISI 4340 steel is defined as the same as the vacuum medium permeability value (m_r=1) since the target temperature is above the Curie point.

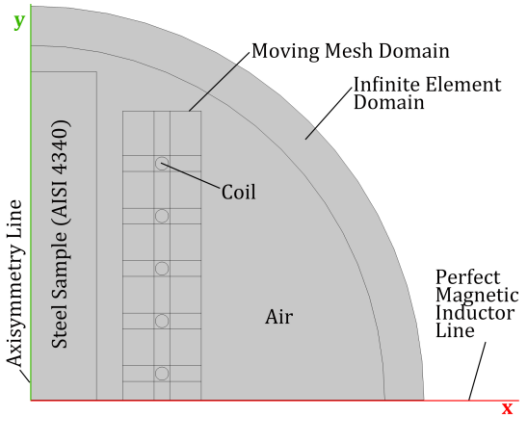


Figure 2. 2-D presentation of the model.

The two-dimensional model created in Comsol software is given in Figure 2. Here, the model is designed axisymmetrically in the y-axis and symmetrically in the x-axis. Thus, processing time is reduced in the analysis.

In the mesh structure of the model; mapped for the moving region, distribution for the infinite region, and free triangular mesh structure for the remaining areas has been used as depicted in Figure 3. In addition, an 8-layer boundary layer is used on the material surface to capture the profile of the magnetic flux.

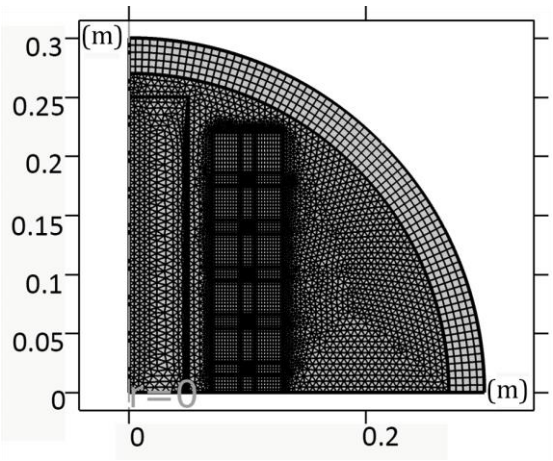


Figure 3. Mesh structure of the model.

The statistics of the mesh structure are given in Table 2.

Table 2. Mesh statistics.

Mesh type	Count
Triangles	5931
Quads	3666
Total Elements	9597

Magnetic field (mf), heat transfer in solid (ht), deformed geometry (dg), boundary partial differential equations in the form of coefficients (cb) and optimization (opt) formulations are used together as physics models in the software. The study that used in the coupled analysis (electromagnetic heating) is carried out in two steps, frequency domain and time dependent modules, respectively. Here, while induction heating is modeled with magnetic field and heat transfer formulations in solid, moving and fixed mesh regions and boundary conditions of motion are defined in deformed geometry and boundary partial differential equations.

2.2. Optimization Model

The aim of the optimization is to obtain the temperature of a certain part of the surface line of the material as close as possible to the austenitizing temperature required for surface hardening while at the same time getting a uniform temperature distribution on the specified line. For this, optimizations have been made by changing the distance of each ring from the center (r) in the first case, and the interval value (z) between the rings in the second case. The defined r and z values are shown in Figure 4. In the optimization, the austenitizing temperature, that is, the target temperature (T_{target}), is determined as 900°C and the target heating time was determined as 2 seconds.

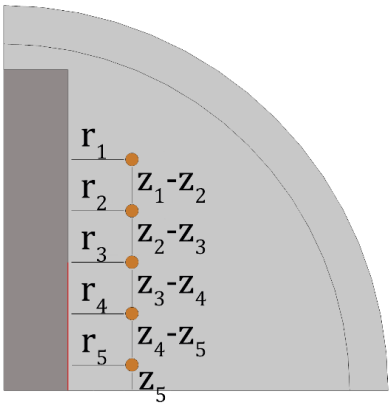


Figure 4. Optimization parameters.

Nelder-Mead is used as the method in the optimization solver. In addition, the required current value to reach 900°C in 2s is determined in the same optimization analysis for both cases. The minimization integral equation used is shown in Equation 1 [19].

$$\frac{1}{L_o}\int_0^{L_o}\left(\frac{T_z}{T_{target}}-1\right)^2 dl \tag{1}$$

Here; L_0 is the size of the target region, T_z is the temperature value at a certain location.

Each coil loop can be moved by the defined $\pm Z_{max}$ and there must be a G_0 gap between adjacent coils as defined in the series of Equation 2. However, the first coil offset (ΔZ_1) has a different lower limit. It is also necessary to add a restriction to the peak value of the current and limit the current to be greater than zero. Peak current value is defined as $I_{max} = 12000$ A.

$$-(S_o - G_o)/2 \leq \Delta Z_1 \leq \Delta Z_{max} \tag{2a}$$
$$-\Delta Z_{max} \leq \Delta Z_2, \ldots, \Delta Z_5 \leq \Delta Z_{max} \tag{2b}$$
$$G_0 \leq (Z_5 - Z_4) \tag{2c}$$
$$G_0 \leq (Z_4 - Z_3) \tag{2d}$$
$$G_0 \leq (Z_3 - Z_2) \tag{2e}$$
$$G_0 \leq (Z_2 - Z_1) \tag{2f}$$
$$I_{min} \leq I \leq I_{max} \tag{2g}$$

3. RESULTS

A series of analyzes is carried out in order to find the required current value for each point of the target surface to be at least 900°C in 2s with a conventional coil of fixed interval and diameter. As a result of the analysis, the current value required to reach the target temperature is determined as 9750 A at a frequency of 100 kHz. The magnetic flux density distribution resulting from the analysis performed with these values is shown in Figure 5. It is seen that the magnetic flux density distribution is concentrated on the outer surface of the sample.

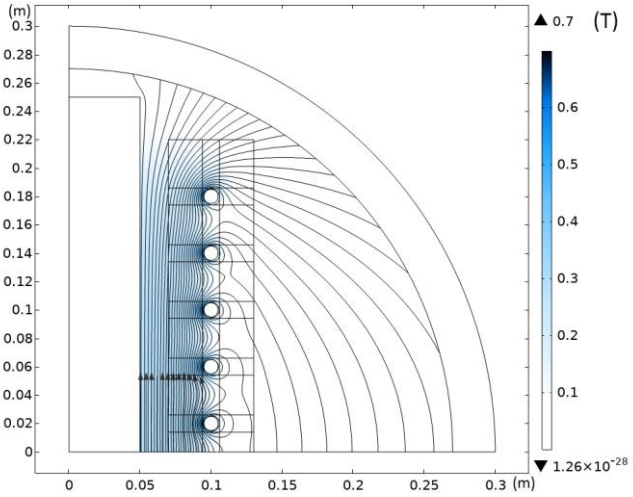


Figure 5. Magnetic flux density distribution.

The temperature distribution obtained in the sample as a result of the coupling analysis of induction heating with the conventional coil is given in Figure 6.

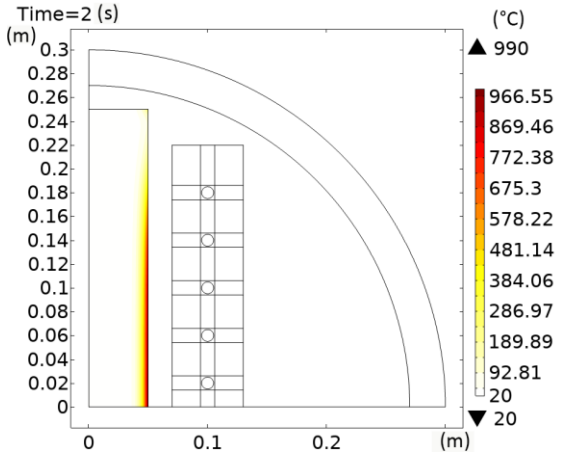


Figure 6. Temperature distribution after heating with conventional coil.

As expected from surface hardening, the temperature rise is high at a shallow depth at the sample surface, but is not affected by the sample core temperature. The graph of variation of the sample surface temperature along the sample surface length is given in Figure 7 for a more detailed examination.

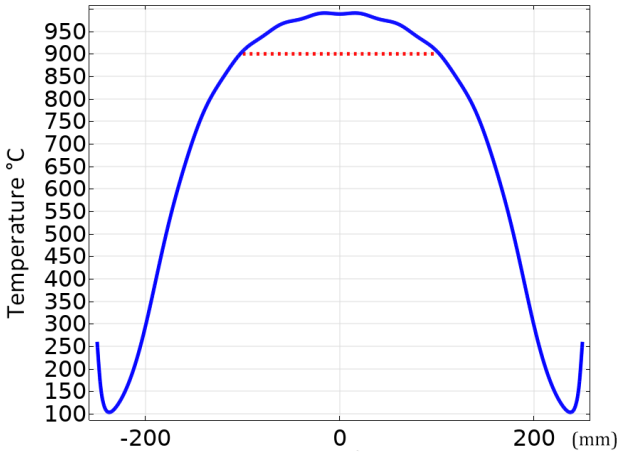


Figure 7. Graph of variation of sample surface temperature along the surface length after heating with a conventional (unoptimized) coil.

The red line on the graph at 900°C represents the targeted heating length (±100 mm) at T_{target}. The temperatures of the boundary of the targeted heating length have been reached T_{target} although high temperature region is in the center of the outer surface of the sample. Deviations from T_{target} up to approximately 90°C at the targeted heating length can be clearly read from the graph.

The temperature distribution obtained in the sample as a result of the optimization made by changing the diameter (r) values of each coil ring is given in Figure 8. The rings in the center move away from the surface and the rings towards the beginning of the coil move closer to the sample surface. After the optimization, the targeted temperature is reached on the sample surface, and only the surface temperature increases as expected from the surface hardening. The temperature at the sample center is around room temperature.

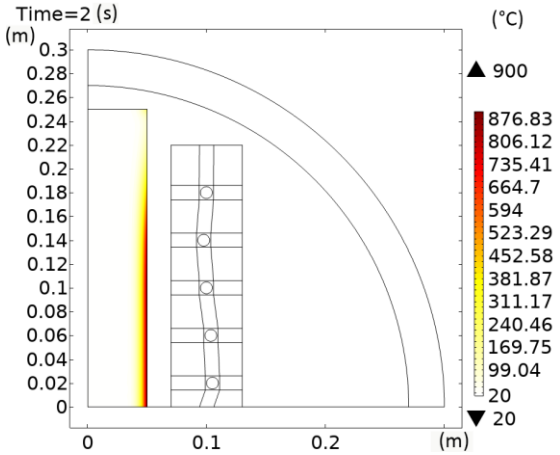


Figure 8. The temperature distribution obtained as a result of the optimization made in the coil diameter.

The graph of variation of the sample surface temperature along the sample surface length is given in Figure 9. When the temperature distribution in the target surface area (the length marked in red) is examined, the temperature of the center of the targeted

heating length (as seen from the graph around 0 mm) has been clearly lowered. The maximum deviation from the T_{target} is determined as $\pm$4°C along the targeted length. The current value required for the surface to reach the T_{target} in 2s has been lowered than unoptimized one and is found to be 9569 A.

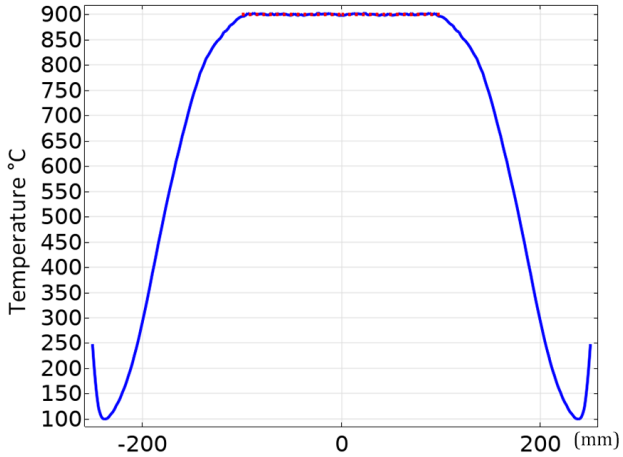


Figure 9. Graph of variation of sample surface temperature along the surface length after heating with the optimized coil diameter.

The temperature distribution obtained in the sample as a result of the optimization of the interval (z) values between the coil rings with the restrictions defined in Equation 2 is given in Figure 10. The intervals of the coil rings have been increased especially positioned towards the center of the targeted length in order to reduce the higher temperature of the surface center. The required temperature rise is achieved only at a shallow depth on the sample surface.

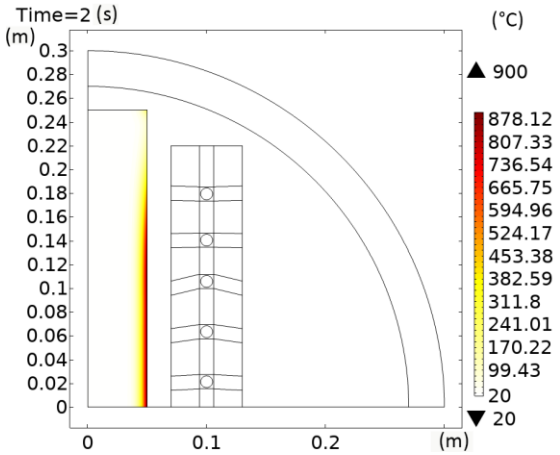


Figure 10. The temperature distribution obtained as a result of the optimization made in the interval between the coils.

According to this temperature distribution, the variation of the sample surface temperature along the sample length is plotted in the graph in Figure 11. When the temperature distribution in the target surface area is examined, the temperature of the

center of the targeted heating length is clearly lowered than unoptimized coil design as seen Figure 7. The temperature deviation from the T_{target} is determined as ± 3°C and the temperature distribution on the sample surface is uniform.

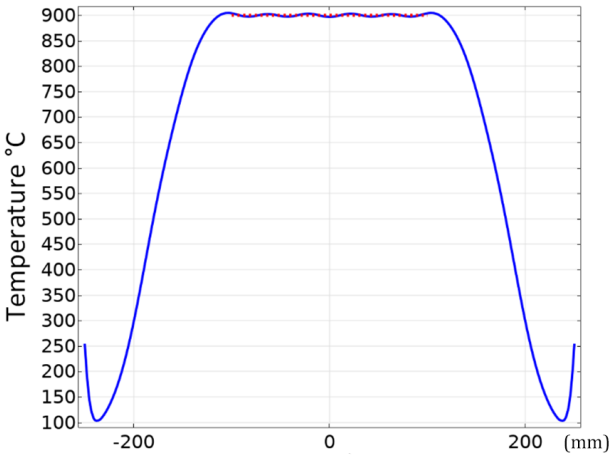


Figure 11. Graph of variation of sample surface temperature along the surface length after heating with the optimized coil interval.

Mei et al. designed two different coil arrangements to get uniform temperature distribution on a graphite susceptor used in chemical vapor deposition reactor. The temperature difference of the susceptor was reduced to 31.9°C and 28.3°C by adding geometric changes to the susceptor [8]. However, in this study geometric changes are not applied to the sample and only the coil is optimized.

The displacement of the coil rings as a result of the optimization and the current values required to reach the target temperature in 2s are summarized in Table 3. Δr values show the displacement of each coil ring in the radial direction and Δz values show the variation of the interval between coil rings after optimization. The number of rings (Ring 1 to Ring 5) increases from the beginning to the center of the coil, as shown in Figure 4. Before optimization, there is no displacement between the interval and diameter of the coil so the displacements values are zero. After the diameter optimization of the coil, the rings in the center, Ring 5 and 4 move away from the surface of the sample, such as 4.88mm, 3.55mm, respectively. The rings (Ring 1, 2 and 3) at the beginning of the coil move closer to the sample surface by 0.22, 2.47 and 0.22mm, respectively. After the interval optimization of the coil, the intervals of the all rings increase to decrease the higher temperature of the surface center in order to achieve uniform temperature distribution. Maximum displacement in the interval of the ring is seen in Ring 3 with 5.75mm. The current value required to reach the T_{target} in 2s is determined as 9750 A. The required current values have been decreased after the diameter and interval optimization of the coils and it is calculated 9569 A and 9630 A, respectively.

Table 3. Post-optimization displacements and required current values of the coil loops.

Situation		Before opt.*	Δr opt.*	Δz opt.*
Displacement (mm)	Ring 1	0	-0.22	0.57
	Ring 2	0	-2.47	0.51
	Ring 3	0	-0.22	5.75
	Ring 4	0	3.55	3.38
	Ring 5	0	4.88	1.26
Current[A]		9750	9569	9630

*optimization

In the induction heating process, the heating intensity affects the homogeneity of the temperature distribution. The faster the heating process at a given region, the worse the homogeneity of the temperature distribution to be achieved [18]. However, with this study, it has been seen that homogeneous temperature distribution can be obtained with the diameter or interval optimizations of the coil in induction analysis performed at a high heating rate of 450°C/s.

4. CONCLUSION

Induction heating of 4340 cylindrical steel samples is modeled with an electromagnetic coil and optimizations have been made to obtain a homogeneous temperature distribution on the sample surface by changing the diameter and interval of each coil ring.

As a result of the induction heating analysis performed on the sample by keeping the diameter and interval of the coil rings constant, the sample temperature deviated by 90°C from the austenitizing temperature which is set as the target temperature. The maximum deviation value from the austenitizing temperature is $\pm$4°C as a result of the optimization made by changing the diameter values of each coil ring. When the interval between the coil rings are optimized, the sample can be heated so that the temperature of the sample surface changes $\pm$3°C from the target temperature. As a result of the optimization, better temperature control of the heat-affected zone is provided and homogeneous temperature distribution in the targeted region is achieved within the targeted time.

Since uniform austenitizing temperature is reached all over the surface, during the quenching, which is the second stage of surface hardening, all parts of the sample surface will cool at the same rate. Accordingly, the same microstructure and hardness will be obtained at every point on the surface after the induction surface hardness process. Thus, the application area of the process develops, especially in applications where high fatigue strength required. For example, rotating shafts in aviation vehicles, gear wheels and also non-rotating beams in static aviation platforms, etc. When the optimized coil geometries are evaluated in terms of usage in manufacturing field, the design in which the coil intervals are changed will be easier to manufacture and more practical in terms of use. After the optimizations have been made in the coils, the current

value required for the sample to reach the austenitizing temperature during the 2s heating period is reduced. Thus, energy savings is achieved in practice with optimization.

REFERENCES

[1] R. Lenhard, M. Malcho, and K. Kaduchova, "Numerical simulation of induction heating thick-walled tubes." *in MATEC Web of Conferences*, EDP Sciences, 2018, 168.

[2] O. Lucia, P. Maussion, E. J. Dede, J. M. Burdio, *Induction heating technology and its applications: past developments, current technology, and future challenges,* IEEE transactions on industrial electronics, **61**(5), 2509-2520 (2014).

[3] V. Rudnev, D. Loveless, and R.L. Cook, *Handbook of Induction Heating*. CRC Press, 2017.

[4] P. R. Stauffer, T.C. Cetas, and R.C. Jones, *Magnetic induction heating of ferromagnetic implants for inducing localized hyperthermia in deep-seated tumors,* IEEE Transactions on Biomedical Engineering, **31**(2), 235-251 (1984).

[5] S. Zinn, S.L. Semiatin, *Elements of induction heating: design, control, and applications.* ASM International, Institute, E.P.R., & Laboratories, B.M.I.C., 1988.

[6] P. Rokicki, *Induction hardening of tool steel for heavily loaded aircraft engine components,* Arch. Metall. Mater. **62**(1), 325-330 (2017).

[7] V. Savaria, F. Bridier, P. Bocher, *Predicting the effects of material properties gradient and residual stresses on the bending fatigue strength of induction hardened aeronautical gears,* International Journal of Fatigue, **85**, 70-84 (2016).

[8] S. Z. Mei, Q. Wang, J. K. Xu, H. B. Yin, H. L. Xiao, C. Feng, L. J. Jiang, X. L. Wang, F. Q. Liu, X. G. Xu, Z. G. Wang, *Simulation and optimization of temperature distribution in induction heating reactor,* Journal of nanoscience and nanotechnology, **18**(11), 7440-7445 (2018).

[9] Z. Li, H. Li, X. Gan, H. Jiang, J. Li, X. Fu, Y. Han, Y. Xia, J. Yin, Y. Huang, S. Hu, *A susceptor with a Λ-shaped slot in a vertical MOCVD reactor by induction heating.* Journal of semiconductors, **35**(9), 092003 (2014).

[10] K. H. Li, H. S. Alotaibi, X. Li, Improvement of temperature uniformity of induction-heated T-shape susceptor for high-temperature MOVPE, arXiv preprint arXiv:1910.02024 (2019).

[11] N. Barka, A. Chebak, J. Brousseau, *Optimization of hardness profile of bearing seating heated by induction process using axisymmetric simulation*, Piers Online, **7**(4), 316-320 (2011).

[12] J. Kucharski, A. Fraczyk, P. Urbanek, *Energy efficient, highly precise cascade dryness control for fibrous tape by induction-based surface heating of a rotating steel cylinder with moving inductors*, Applied Sciences, **12**(1), 261 (2021).

[13] A. Fraczyk, J. Kucharski, *Surface temperature control of a rotating cylinder heated by moving inductors,* Applied Thermal Engineering, **125**, 767-779 (2017).

[14] J. Barglik, A. Smalcerz, R. Przylucki, I. Doležel, *3D modeling of induction hardening of gear wheels*, Journal of Computational and Applied Mathematics, **270**, 231-240 (2014).

[15] Y. Q. Zhao, Y. Han, Y. Xiao, *An asynchronous dual-frequency induction heating process for bevel gears*, Applied Thermal Engineering, **169**, 114981 (2020).
[16] C. Ajus, S. S. M. Tavares, M. R. Silva, R. R. A. Corte, *Magnetic properties and retained austenite quantification in SAE 4340 steel*, Materia-Rio De Janeiro, **14**(3), 993-999 (2009).
[17] Y. Wang, X. Hu, M. Jiang, J. Wang, M. Wei, L. Zhang, *Temperature field characterization and optimization of temperature field distribution in pipe lining process based on electromagnetic induction heating system*, Case studies in thermal engineering, **28**, 101609 (2021).
[18] O. Okman, Free forming of locally induction heated specimens. Middle East Technical University, 2005.
[19] W. Frei, "3 Ways to Optimize the Current in Electromagnetic Coils", 2017 [Online]. Available: https://www.comsol.com/blogs/3-ways-to-optimize-the-current-in-electromagnetic-coils/. [Accessed: June 20, 2022].

To Cite This Article: Y. Yamac, B. Ozcelik, *Optimization of Induction Heating Coil in the Surface Hardening Process,* Journal of Aeronautics and Space Technologies **16**(1), 1-14 (2023).

VITAE

Yalın Yamaç received his B.Sc. degree in Mechanical Engineering from Faculty of Engineering, Pamukkale University, Turkey in 2016. He received his M.Sc. degree in Mechanical Engineering from Kahramanmaras Sutcu Imam University, Turkey in 2019. He is currently a Ph.D student and working at KSU as a Research Assistant.

Beril Özçelik received her B.Sc., M.Sc. and Ph.D degree in Mechanical Engineering from Istanbul Technical University, Turkey in 2005, 2007 and 2014, respectively. She is currently working at the Faculty of Enginering and Architecture in Kahramanmaras Sutcu Imam University as an assistant professor.